Journal of the Serbian Chemical Society
JSCS-info@shd.org.rs • www.shd.org.rs/JSCS
J. Serb. Chem. Soc. 82 (2) 227–240 (2017)
JSCS–4961
UDC 620.4+541.183+549.67:66.099.72:
620.28.002.68:536.5(497.2)
Original scientific paper

Room temperature zeolitization of boiler slag from a Bulgarian thermal power plant

RADOST D. PASCOVA*, VALERIA B. STOYANOVA and ANNIE S. SHOUMKOVA

Institute of Physical Chemistry "Rostislaw Kaischew" – Bulgarian Academy of Sciences, Acad. G. Bonchev str., Bl. 11, Sofia 1113, Bulgaria

(Received 7 august, revised 27 September, accepted 3 October 2016)

Abstract: A simple and cost-effective method was applied for the synthesis of zeolite composites utilising wet bottom boiler slag from the Bulgarian coal--fired thermal power plant "Sviloza", near the town of Svishtov. The method consisted of a prolonged alkali treatment at room temperature of this waste. Experimental techniques, such as scanning electron microscopy, energy-dispersive X-ray and X-ray diffraction analyses, are employed to characterize the initial slag and the final products with respect to their morphology, and elemental and mineral compositions. The composites synthesized in this way contained two Na-type zeolite phases: zeolite X (type FAU) and zeolite Linde F (type EDI). The zeolited products and the starting slag were tested as adsorbents for a textile dye (Malachite Green) from aqueous solutions. In comparison with the initial slag, the zeolite composite possessed substantially better adsorption properties: it almost completely adsorbs the dye in much shorter times. The results of this investigations revealed a new, easy and low cost route for recycling boiler slag into a material with good adsorption characteristics, which could find different applications, *e.g.*, for purifying polluted waters, including those from the textile industry.

Keywords: waste recycling; zeolite X; zeolite Linde F(Na); dye removal; adsorption.

INTRODUCTION

Boiler slag is an incombustible vitreous waste product from coal-fired thermal power plants (TPP) equipped with a slag-tap or cyclone type furnaces.[1,2] Due to the high combustion temperatures (1350–1500 °C) reached in these type of furnaces, the bottom ash is in a molten state before its removal. After rapid quenching of this molten residue into water, a glassy grain mass is obtained that fractures into particles with irregular shapes and sizes up to 20 mm.[1,2]

* Corresponding author. E-mail: rpascova@hotmail.com
doi: 10.2298/JSC160807091P

The composition of boiler slag mainly depends on the coal source and the combustion conditions. Generally, it is composed of silica, alumina, iron oxides, small amounts of calcium and magnesium oxides, sulphates, and some other compounds. According to recent information, about 100 million tonnes of coal combustion by-products (bottom and fly ashes, boiler slag, *etc*.) are produced in Europe and approximately 780 million tonnes per year worldwide.[1–4]

Boiler slag represents about 2 % of the total quantity of these coal combustion products, *i.e.*, the European power plants produce about 2 million t of slag per year. In the old European partner countries, the utilization rate of this slag reaches 100 %.[1] About 45 % is used as blasting grid, about 30 % in road construction, 10 % as aggregates in concrete and about 5 % for grouting and drainage.[1,2,4] However, regarding the other European countries, there is no detailed information concerning the re-use rate and fields of application of this waste. Boiler slag also finds application as roofing shingle granules, or it can be spread on icy roads for traction control.[1,2,4] However, in all these applications, the boiler slag is used as an inert ingredient and not as a resource for the synthesis of new products with useful properties, in contrast to the fly and bottom ashes.[1–5] In respect to the latter, there is increased interest in their recycling utilizing them as a raw material for the synthesis of zeolite composites.[3,6–18] Due to the specific zeolite structure, such composites are used in a wide range of environmental engineering processes, such as for the removal of heavy metals, oil-derivative contaminants or of other pollutants from effluent waters.[3,6–10,13–15,18] Boiler slag could also be a useful raw material in this respect. Containing large amounts of Si and Al in an easy soluble glassy form, this waste product is exceptionally appropriate for the alkali-activated synthesis of different zeolite composites.

Usually, the synthesis of zeolites from different wastes is performed under hydrothermal conditions, which really accelerate the zeolitization but, simultaneously considerably raise the recycling costs.[3] Successful experiments for zeolite synthesis at low temperatures and under atmospheric pressure have been performed for years.[19–22] However, in all these investigations, pure chemicals were exclusively used.[19–22] Only recently, several investigations were performed for recycling fly ashes[23–27] and other waste products[28] into materials rich in zeolite phases at low temperatures. Experiments for the room temperature zeolitization of fly ashes from six different Bulgarian TPPs were also performed (unpublished results). To the best of our knowledge, low temperature synthesis routes have not hitherto been applied for the zeolitization of boiler slag.

For this reason, the aim of the present study was to demonstrate the feasibility of boiler slag zeolitization at room temperature and in this way to propose a simple and cost-effective method for its recycling. With the view to future application, the adsorption behaviour of the synthesized zeolite composite was investigated with respect to a textile dye.

EXPERIMENTAL

The slag used in the present study was collected from the Bulgarian coal-fired TPP "Sviloza", near the town of Svishtov. Prior to the synthesis, the slag was screened to obtain two fractions: the first one with particle sizes smaller than 0.2 mm (S-fraction) and the second one with larger particle sizes between 2 and 5 mm (L-fraction).

Details on zeolitization experiments are given in Supplementary material to this paper.

The phase composition of all samples was investigated employing a Philips PW 1050 automatic powder diffractometer using Cu-K_α filtered radiation and Bragg–Brentano geometry. The patterns were recorded in the 2θ interval from 6 to 85°. Samples with equal masses and identical sample holders were used in all XRD measurements. The identification of all crystalline phases was performed by the X'Pert HighScore 3.0d software (2011 PANalytical B.V., The Netherlands) and the collection of X-ray patterns of the International Zeolite Association.[29]

The morphology and the elemental composition of the initial slag and of the reaction products were investigated by SEM, using a JEOL JSM6390 microscope, equipped with an EDX analyzer, Oxford Instruments. Information about the integral elemental composition of the samples was obtained taking a few spectra at low magnification (30×) from their surface. The elemental composition of crystals of a given morphology or of the amorphous precipitates formed during the alkali treatment was determined using "in point" analysis of at least ten individual objects. In the latter case, the analyses were performed at substantially higher magnifications (100000–300000×).

Information for some other properties of the slag from the same TPP is available,[17] *e.g.*, data on the elution behaviour of the slag under the influence of different solvents, on the changes in the structure and chemical composition of the slag under atmospheric conditions, *etc.*

The adsorption properties of the solid reaction products and of the initial slag were investigated using an aqueous solution of Malachite Green (MG). MG is an organic compound ($C_{23}H_{25}ClN_2$) used for the colouring of silk, leather, paper, *etc*. It often appears as a pollutant in effluent waters of the respective industries, including the aquaculture industry.[30,31] All adsorption measurements were realised using a 1200 Series UV spectrophotometer (Cole Palmer Instruments, UK).

RESULTS

X-Ray diffraction analysis

The X-ray diffraction patterns of the initial slag and of the filtered reaction products after 210 and 410 days of alkali treatment of the S- and L-fractions are presented in Fig. 1. The initial slag was fully amorphous, as indicated by the presence of a large amorphous halo in its pattern. A large amorphous halo was also clearly visible in the XRD pattern of the respective L-fraction samples taken after 210 and 410 days of treatment. Moreover, the latter two spectra are almost identical to that of the initial slag; the only difference is the presence of two unidentified small peaks in the spectrum of the sample L410. This means that even 410 days of alkali activation were not enough for initiating the zeolitization of the coarser L-fraction.

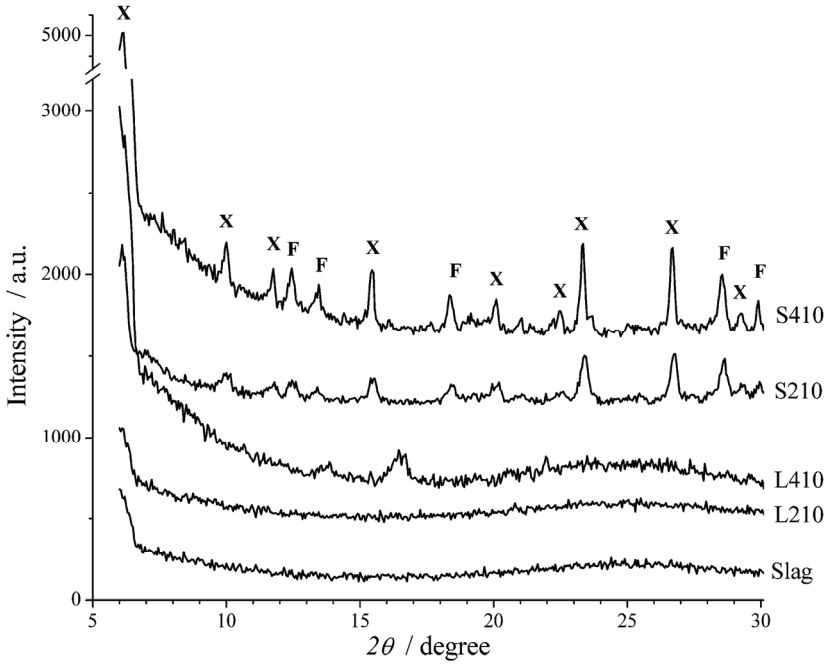

Fig. 1. X-Ray diffraction patterns of the initial slag and of the reaction products of the S- and L-fractions. For the meaning of the sample codes under each pattern, see the text.

In contrast to the initial slag and the L-fraction samples, both spectra of the S-fraction (taken after 210 and 410 days) show many diffraction peaks, indicating the formation of different crystalline phases. After thorough analysis, the presence of zeolite X (low silica Na-LSX, type FAU, ref. code 98-008-5620, $Na_{96}(Al_{96}Si_{96}O_{384})(H_2O)_{384.3}$) was identified. Its most intensive peak was determined at 2θ 6.10° for the S210 sample, and at 2θ 6.15° for the S410 sample. In addition, a second zeolite phase was detected in the above samples, most probably zeolite F (Linde F-Na, type EDI, ref. code 98-000-6272, $Na_5(Al_5Si_5O_{20})(H_2O)_9$). Its most intensive peak was determined at 2θ 12.45° for both S-samples. Small amounts of other two non-zeolitic silicate crystalline phases were also found, namely Fe-containing Akermanite (ref. code 98-009-4154, $Ca_2Mg_{0.55}Fe_{0.45}Si_2O_7$), and Combeite (ref. code 96-900-7718, $Ca_{12}Na_{12}Si_{18}O_{54}$).

Since the XRD patterns were recorded using the same apparatus and under the same conditions, it was possible to give at least a semi-quantitative estimation of the relative content of the two zeolite phases (X and F) formed after 210 and 410 days of treatment of the S-fraction. For this purpose, the heights H of their most intensive peaks were compared and the result is presented in Fig. S-1 of the Supplementary material.

As seen in Figs. 1 and S-1, the content of the zeolite X phase was significantly higher than that of zeolite F for both investigated treatment times. Moreover, the ratio between the contents of the X and F phases increased with treatment time from about 4.3 after 210 days to about 5.4 after 410 days. Therefore, the main crystalline phase in both samples (S210 and S410) was zeolite X. This result was also supported by the SEM investigations reported in the following section.

Morphology of the reaction products

Typical images of the reaction products formed during the alkali treatment of fractions L and S are shown in Figs. 2 and 3.

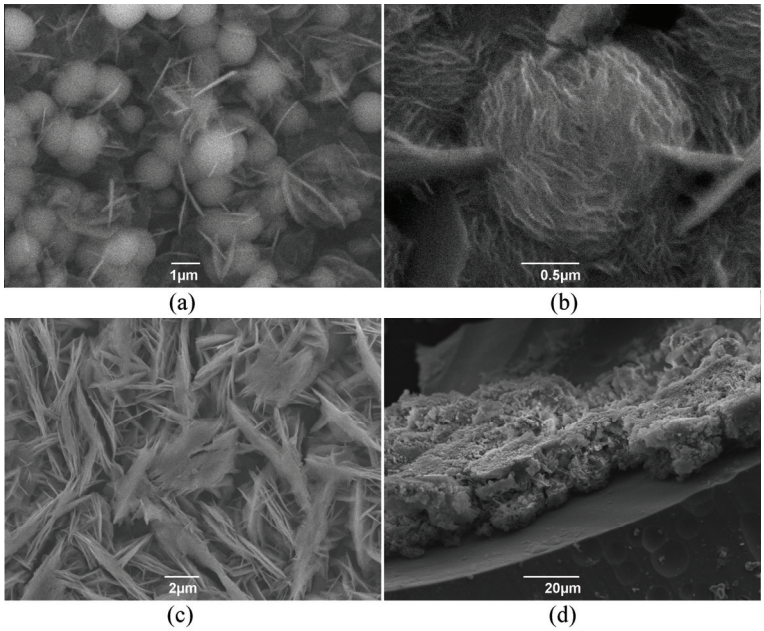

Fig. 2. Self-organization of the alumino-silicate gel into ball-like (a, b) and thread-like (a, b, c) amorphous precipitates, and into thick amorphous layer (d) on the surfaces of the L-fraction slag grain after 410 days of alkali treatment.

In the case of the coarser L-fraction, variously shaped precipitates, *e.g.* ball--like ones (Fig. 2a and b) or thread-like ones (Fig. 2a–c) with different sizes were visible in all the studied samples. A general view of the structure of a thick gel layer situated on the surface of a non-dissolved glassy slag particle is given in Fig. 2d. Considering the results of the XRD analysis, all these precipitates should be amorphous. They are most probably the products of self-organization of the alumino-silicate gel formed during the alkali-activated dissolution of the glassy slag.[32]

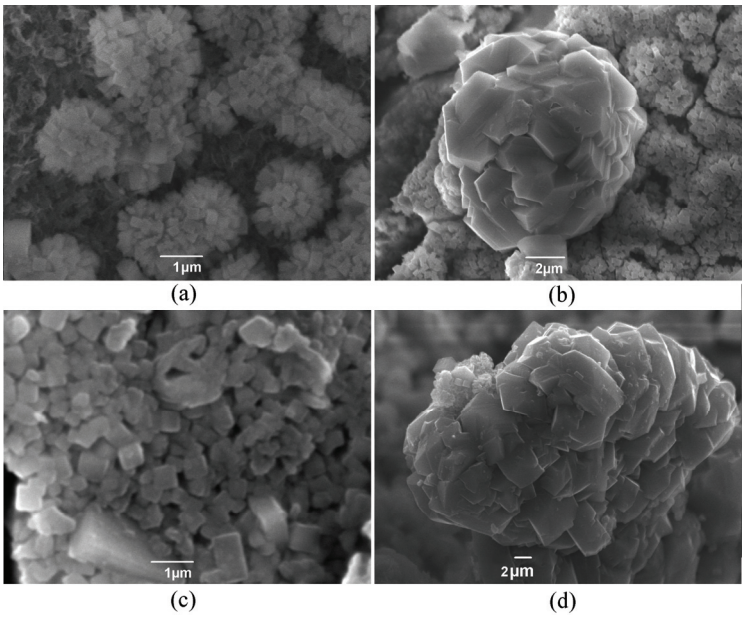

Fig. 3. Morphology of zeolite F (a, c) and zeolite X (b, d) crystallites formed after 144 days (a, b), and after 410 days (c, d) of treatment of the finer slag S.

However, regarding the finer S-fraction, the situation is quite different. The results of detailed SEM – investigations show that after 144 days of treatment, two morphologically different types of crystallites could be distinguished, *i.e.*, bundles of prismatic crystallites, a few micrometers in length and with submicron square section of the individual prisms (Fig. 3a), and bigger aggregates of monolithic octahedral crystals with well-developed flat faces (Fig. 3b). These two types of crystallites were observed up to the latest stages of alkali treatment (see Fig. 3c and d). Considering the morphology of the observed crystalline phases, as well as the results from X-ray diffraction analysis and of other investigations, the aggregates of the larger octahedral crystallites were identified as zeolite X,[14,18,21–25,33–37] while the bundles of prismatic crystallites are most probably zeolite Linde F(Na).[38–40]

The comparison of Fig. 3a with Fig. 3c, and of Fig. 3b with Fig. 3d, clearly shows that the crystallites of both zeolite phases had increased in size. Using a series of SEM micrographs, it was estimated that the square section of the prismatic zeolite F crystallites and of the bundles of these crystallites increased nearly two times from 0.1–0.2 up to 0.4 μm, and from 1–2 up to 4–5 μm from the 144 to the 410 day of treatment, respectively. Due to the specific morphology of the bundles, it is difficult to estimate the length of the individual prismatic crystals. During the same time interval, the individual monolithic crystals of zeolite X increased from 1–2 μm up to 5–6 μm while the aggregates of the same crystal-

lites grow from the initial 5–6 μm up to 30–40 μm. This means that the growth rate of zeolite X crystals was substantially higher than that of the zeolite F phase.

During the initial stages of alkali treatment (up to 210 days), amorphous precipitates (mainly threads) could be seen together with zeolite aggregates (Fig. 4a and b).

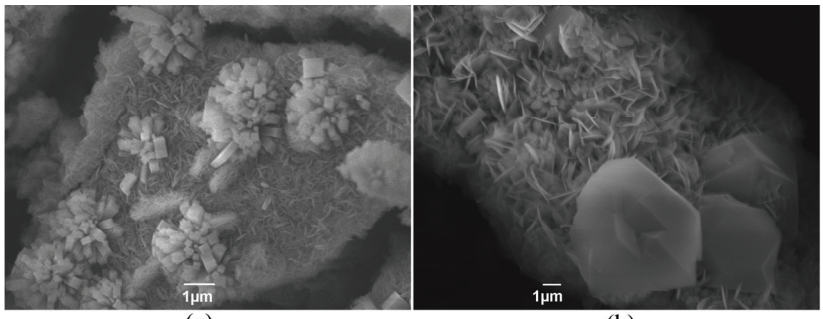

Fig. 4. Illustration of the simultaneous presence of amorphous alumino-silicate precipitates and crystals of zeolite F (a) and zeolite X (b) during the initial stages of treatment of slag fraction S.

It was found that the content of amorphous precipitates considerably decreased with the time, while that of the zeolite phases increased. This fact could be considered as an indirect indication that the zeolite phases grew at the expense of the thermodynamically more unstable amorphous precipitates.[32] However, due to the low content of the latter, there was no indication for the existence of amorphous halo in the XRD pattern of the respective S fraction sample (see the pattern of the S210 sample in Fig. 1).

The changes in the surface concentration of the crystal aggregates of both the zeolite phases with treatment time are illustrated in Fig. 5.

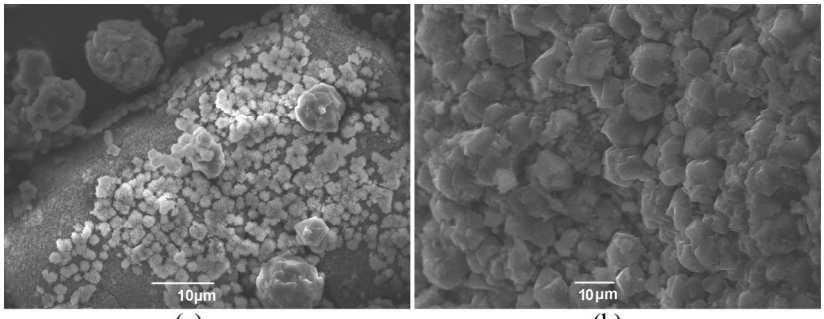

Fig. 5. SEM images from the surface of zeolite composite samples obtained after 144 (a) and 410 days (b) of alkali activation of the finer slag fraction S.

Initially, aggregates of zeolite X are rarely observed, while the surface concentration of bundles of the zeolite F crystallites is very high (see Fig. 5a). This indicates that the nucleation rate of zeolite F is substantially higher than that of zeolite X. Simultaneously, the bigger sizes of the individual X zeolite crystallites show that the latter grew significantly faster than the numerous smaller zeolite F crystallites, as has already been mentioned in the discussion of Fig. 3.

However, the situation became entirely different in the advanced stages, *i.e.*, the concentration of zeolite X aggregates significantly increased. This evidences that the conditions in the reaction system were obviously changed in a way favouring the nucleation of zeolite X. As a result, the combination of high nucleation and growth rates of the zeolite X phase leads to an almost full coverage of the surface of the slag particles by crystals of this phase in the latter treatment stages (see Fig. 5b).

Elemental composition

The data for the integral elemental composition, obtained by integral EDX analysis of the respective samples at low magnification, for the initial slag together with those for the reaction products after different treatment times (144, 210 and 410 days) of the finer fraction S are summarized in Table I. Table I also contains the averaged elemental composition of the zeolite crystals (X and F) formed after 410 days of treatment of fraction S. For comparison, the averaged composition of the amorphous precipitates, obtained after 410 days of activation of the coarser fraction L, is also given.

TABLE I. Elemental composition of the initial slag and of the reaction products after different times of treatment. The Si to Al ratio is given in the last column.

Sample	Composition, at. %										Si/Al
	O	Na	Al	Si	Ca	Fe	K	Mg	Ti	S	
Slag	61.9	0.8	7.7	15.0	4.4	5.7	1.9	0.9	0.0	1.7	1.95
S144	71.8	3.3	7.2	9.3	2.8	3.9	0.3	1.2	0.2	0.0	1.29
S210	70.1	4.5	7.4	9.6	2.9	4.0	0.3	1.0	0.2	0.0	1.30
S410	55.8	7.1	10.5	14.2	3.6	6.6	0.7	1.2	0.3	0.0	1.35
Zeolite X (S410)	61.7	7.7	13.4	13.8	3.1	0.3	0.0	0.0	0.0	0.0	1.03
Zeolite F (S410)	54.3	6.7	11.5	13.6	4.9	8.6	0.2	0.2	0.0	0.0	1.18
Amorphous precipitates (L410)	59.6	0.2	5.0	10.4	7.0	11.6	0.3	5.6	0.2	0.1	2.08

The contents of Na, Al, Si, K, Mg, Ca, and Fe in the reaction products as a function of the treatment time of fraction S are presented in Fig. S-2 of the Supplementary material. The contents of oxygen as well as those of some trace elements (Ti, S) are not included.

For better illustration, Fig. S-2a gives the changes with time of alkali activation for the elements present at higher concentrations (Si, Al and Na), while Fig. S-2b gives the corresponding data for those present in lower concentrations

(K, Mg, Ca and Fe). As seen in Table I and Fig. S-2a, the content of Na monotonously increased with the treatment time. Taking into account the EDX analyses of the individual crystallites and the results of the XRD investigations, this effect is obviously due to incorporation of sodium into the structure of the two zeolite phases – X and F. Simultaneously, after an initial decrease during the first 144 days of alkali activation, the concentrations of Si and Al began to increase. In the advanced stages, the silicon content gradually reached a value almost equal to that in the initial slag, while the aluminium concentration became about 40 % higher than that in the untreated slag. As a result, the ratio between the concentrations of silicon and aluminium decreased from 1.95 in the initial slag to 1.35 in the reaction products after 410 days of alkali activation.

With respect to the elements present at lower concentrations, it was observed that the contents of Fe, K and Ca initially decreased at almost equal rates (see Table I and Fig. S-2b). During the latter treatment stages, the concentrations of K and Ca slightly increased remaining, however, substantially lower than those in the initial slag. This means that only parts of these elements were incorporated into the structure of the respective solid reaction products, while the remaining parts obviously formed water-soluble products under the influence of NaOH. On the contrary, the content of Fe reached a value that was even slightly higher than that in the initial slag. During all treatment stages, the concentration of Mg remained almost constant.

The data on the contents of the same elements as in Fig. S-2 in the initial slag and in the solid products obtained after 410 days of alkali treatment of slag fraction S (Sample S410) are summarized in Fig. S-3 of the Supplementary material.

The concentrations of the respective elements in the crystallites of the two zeolite phases (Zeo X and Zeo F) formed after the same treatment time from fraction S are also shown in Fig S-3. Both zeolite phases were characterized by substantially higher concentrations of sodium (about 10 times) and of aluminium (about 2 times) than those in the initial slag. The main difference between the two zeolite phases was the presence of more than 8 at. % iron in the zeolite F crystallites and only traces of iron in the zeolite X crystallites. This indicates the preferential incorporation/adsorption of iron into/onto the zeolite F crystallites. The zeolite X crystallites are characterized by slightly higher sodium and lower calcium contents and with an about 15 % higher Si/Al ratio as compared with the zeolite F crystallites.

Synthesis yield

The trends in dissolution and growth of the solid reaction products, *i.e.*, of their yield, were followed by taking aliquots from the respective alkali suspensions investigated. It was established that the content of reaction products dec-

reased during the first 100 days for fraction S, and during the first 200 days for fraction L. This decrease is obviously a result of the dissolution of the initial slag under the influence of NaOH. Subsequently, the quantity of reaction products began to increase due to the formation of new crystalline and amorphous phases in the alkali activated suspensions. In the case of the fraction S, the yield of the composite material mainly consisting of valuable zeolite phases reached 140 % after 410 days of alkali treatment. For the same treatment time, the yield of the fraction L is not only substantially lower (105 %) but it represented a mixture of amorphous precipitates and still non-dissolved glassy slag grains.

Adsorption properties

The adsorption of Malachite Green was investigated with respect to the initial slag and the sample S410, which was characterized with the highest degree of zeolitization. The calibration curve used in this investigation was plotted using aqueous solutions of MG with known concentrations. These solutions were prepared by diluting the initial dye stock solution (20 mg L^{-1}) with deionised water. Their absorbance was measured at room temperature and at the wavelength of maximum absorbance of MG (617 nm).

To follow the adsorption kinetics, two sets of suspensions were prepared using a solution of MG with concentration of 10 mg L^{-1} and adding 3 g L^{-1} of the initial slag or of the zeolite composite (sample S410). The measurements were performed at room temperature and for contact times reaching up to 48 h. All suspensions were stirred during the respective contact time, filtered, and the absorbance $A(t)$ of the filtrates was measured. The thus obtained $A(t)$ values were used for calculating the dye removal R according to the following equation:

$$R = \frac{A_0 - A(t)}{A_0} 100 \quad (1)$$

where A_0 is the absorbance of the initial MG solution.

The R *vs.* t dependences obtained with the two sets of suspensions are presented in Fig. 6. As could be seen, the initial slag hardly reached about 70 % of dye removal after 24 h and, more importantly, this was its maximum removal efficiency. In contrast, the zeolite composite (sample S410) removed the dye faster and to a higher percentage as compared to the initial slag. The degree of MG removal increased to nearly 70 % after the first 5 min of contact with the composite and up to 98 % during the next 5 h. This high degree of dye removal was for expectation considering its relatively high content of valuable porous zeolite phases with a well-developed active specific surface.

DISCUSSION

In interpreting the experimental results, the fact that zeolite formation even in the case of crystallization from pure chemical reagents is still not well

understood[20,21,32] has to be taken into consideration. The problem becomes more complicated with respect to zeolitization processes in heterogeneous reaction systems, such as the one investigated in the present study. The processes occurring in such systems are very complex; they simultaneously include dissolution of the multi-component slag, gel formation from the dissolved alumino-silicate species and its self-structuring, followed by nucleation and growth of zeolite and other crystalline phases.[20,21,32] As is well known, factors, such as temperature, composition of the initial slag and the concentration of NaOH in the activation solution can significantly influence these processes. This hinders the possibility for predicting the synthesis results, such as the type of zeolites formed, their nucleation and growth kinetics, and their yield. Therefore, experiments and the simultaneous application of different analytical techniques is the only way to receive reliable information. For this reason, various methods like XRD and EDX analyses, SEM and spectrophotometry were used in the present study for investigating the processes occurring during the alkali activation treatment of the slag. It was found that zeolite X was the main crystalline phase formed during the alkali treatment of boiler slag at room temperature. Here, it is interesting to note that the same zeolite phase (zeolite X) was also identified after employing similar synthesis conditions to several fly ashes of different in origin, *i.e.*, six from Bulgarian TPPs (unpublished results) and from two Polish ones.[23,24]

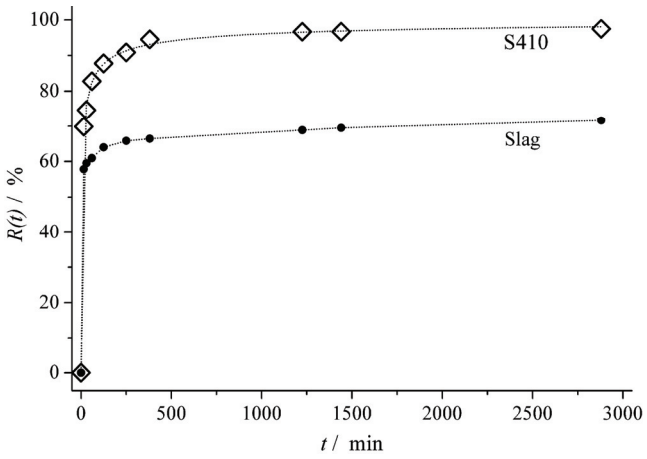

Fig. 6. Dye removal *R versus* the contact time *t* using the initial slag and the zeolite composite (S410).

One of the main results of the present investigation was that the zeolitization occurred only with the finer slag fraction (S). In contrast, only the formation of amorphous precipitates was observed in the case of the coarser fraction L. These differences in the behaviour of the two slag fractions (slower or faster dissolution, different yield, structure and composition of the final products) are most

probably the result of the higher specific surface of the finer S-fraction as compared with that of the coarser L-fraction.[41,42] Hence, the slag grain size, *i.e.*, the specific slag surface, is of substantial importance for the zeolitization process. In addition, it has to be taken into consideration that the grains of the finer fraction had a higher surface roughness and a higher concentration of different defects, such as scratches and cracks.[41,42] This additionally enhanced the reactivity of the slag and thus influenced both the zeolitization process and adsorption properties of the synthesized zeolite composites.

CONCLUSIONS

The results of present study show that employing alkali treatment at room temperature to boiler slag it is possible to synthesize composite materials with a high content of valuable zeolite phases. Thus, the boiler slag could be recycled into a new useful product that could find different applications, *e.g.*, as an adsorbent for the purification of industrial effluent waters, as was demonstrated by the present adsorption investigations with respect to Malachite Green dye. An important prerequisite for achieving high zeolitization degree is the use of finely milled slag.

This method for boiler slag zeolitization is simple and energetically effective, needs no high investments and could be considered as a promising and environmental friendly novel route for the recycling of this waste.

SUPPLEMENTARY MATERIAL

Details on zeolitization and additional figures concerning XRD peaks and composition of the initial slag and reaction products are available electronically at the pages of journal website: http://www.shd.org.rs/JSCS/, or from the corresponding author on request.

Acknowledgments. The authors express their gratitude to their colleagues from the Institute of Physical Chemistry, Assoc. Prof. G. Avdeev for carrying out the XRD measurements, and Assoc. Prof. S. Atanasova and I. Piroeva for the SEM-EDX investigations.

ИЗВОД

ЗЕОЛИТИЗАЦИЈА КОТЛОВСКОГ МУЉА ИЗ ЈЕДНЕ ТЕРМОЕЛЕКТРАНЕ У БУГАРСКОЈ НА СОБНОЈ ТЕМПЕРАТУРИ

RADOST D. PASCOVA*, VALERIA B. STOYANOVA и ANNIE S. SHOUMKOVA

Institute of Physical Chemistry "Rostislaw Kaischew" – Bulgarian Academy of Sciences, Acad. G. Bonchev str., Bl. 11, Sofia 1113, Bulgaria

Примењен је једноставан и исплатив метод за синтезу зеолитских композита коришћењем влажног муља са дна котла термоелектране на угаљ "Свилоза", поред града Свиштова у Бугарској. Метод се састоји од продуженог алкалног третмана овог отпада на собној температури. За карактеризацију почетног муља, као и коначних продуката у смислу њихове морфологије, елементалног и минералног састава коришћене су методе сканирајуће електронске микроскопије (SEM), рентгенске анализе (EDX) са дисперзијом енергије и рентгенске дифракције (XRD). Овако синтетисани композити садрже две фазе натријумских зеолита: зеолит X (тип FAU) и зеолит Linde F (тип EDI).

Зеолитизовани продукти, као и почетни муљ испитани су као адсорбенси текстилне боје (малахитно зелено) из водених раствора. У поређењу са почетним муљем, зеолитски композит поседује суштински боље адсорпционе особине: скоро потпуно адсорбује боју за знатно краће време. Резултати ових истраживања откривају нову и исплативу путању за рециклирање котловског муља, претварањем у материјал са добрим адсорпционим карактеристикама, за којег би се могле пронаћи разне примене, нпр. за пречишћавање загађених вода, укључујући оне из текстилне индустрије.

(Примљено 7. августа, ревидирано 27. септембра, прихваћено 3. октобра 2016)

REFERENCES

1. Joint EURELECTRIC/ECOBA Briefing: The Classification of Coal Combustion Products under the revised Waste Framework Directive (2008/98/EC, http://www.ecoba.com/ /evjm,media/downloads/ECOBA_EURELECTRIC_Commission_Brief_June_2011.pdf (23.05.2016)
2. *User Guidelines for Waste and By-product Materials*, in *Pavement Construction*, Publ. Numb. FHWA-RD-97-148, Federal Highway Administration, 1998
3. X. Querol, N. Moreno, J. C. Umana, A. Alastuey, E. Hernandez, A. Lopez-Soler, F. Plana, *Int. J. Coal Geol.* **50** (2002) 413
4. B. W. Ramme, M. P. Tharaniyil, *Coal Combustion Products Utilization Handbook*, 3rd ed., We Energies, Wisconsin Electric Power Company, Milwaukee, WI, 2013
5. N. L. Hecht, D. S. Duvall, in *Characterization and Utilization of Municipal and Utility Sludges and Ashes*, Vol. III, National Environmental Research Center, U.S. Environmental Protection Agency, 1975
6. M. Ahmaruzzaman, *Prog. Energy Combust. Sci.* **36** (2010) 327
7. R. S. Blissett , N. A. Rowson, *Fuel* **97** (2012) 1
8. A. Shoumkova, Res. Bull. Aus. Inst. High Energetic Mater. **2** (2011) 10–70
9. N. Moreno, X. Querol, C. Ayora, C. F. Pereira, M. Janssen-Jurkovicova, *Environ. Sci. Technol.* **35** (2001) 3526
10. C. D. Woolard, J. Strong, C. R. Erasmus, *Appl. Geochem.* **17** (2002) 1159
11. D. Vucinic, I. Miljanovic, A. Rosic, P. Lazic, *J. Serb. Chem. Soc.* **68** (2003) 471
12. M. Inada, Y. Eguchi, N. Enomoto, J. Hojo, *Fuel* **84** (2005) 299
13. S. Wang, M. Soudi, L. Li, Z. H. Zhu, *J. Hazard. Mater.,* B **133** (2006) 243
14. C. Wang, J. Li, L. Wang, X. Sun, J. Huang, *Chin. J. Chem. Eng.* **17** (2009) 513
15. T. E. M. de Carvalho, D. A. Fungaro, C. P. Magdalena, P. Cunico, *J. Radioanal. Nucl. Chem.* **289** (2011) 617
16. A. Shoumkova, V. Stoyanova, Ts. Tsacheva, *Compt. Rend. Acad. Bulg. Sci.* **64** (2011) 937
17. P. Petrov, *PhD Thesis*, HTMU, Sofia, 2011, http://mmu2.uctm.edu/science/files/ /avtoreferat_Petar%20GPetrov.pdf
18. J. de C. Izidoro, D. A. Fungaro, J. E. Abbott, S. Wang, *Fuel* **103** (2013) 827
19. L. B. Sand, A. Sacco Jr., R. W. Thompson, A. G. Dixon, *Zeolites* **7** (1987) 387
20. S. Mintova, N. H. Olson, V. Valtchev, T. Bein, *Science* **283** (1999) 958
21. V. P. Valtchev, K. N. Bozhilov, *J. Phys. Chem., B* **108** (2004) 15587
22. X. Zhang, D. Q. Tong, J. J. Zhao, X. Y. Li, *Mater. Lett*. **104** (2013) 80
23. A. Derkowski, W. Franus, H. Waniak-Nowicka, A. Czimerova, *Int. J. Miner. Process.* **82** (2007) 57
24. W. Franus, *Pol. J. Environ. Stud.* **21** (2012) 337

25. C. Belviso, F. Cavalcante, F. J. Huertas, A. Lettino, P. Ragone, S. Fiore, *Micropor. Mesopor. Mater.* **162** (2012) 115
26. D. Zgureva, S. Boycheva, Synthesis of Highly Porous Micro- and Nanocrystalline Zeolites from Aluminosilicate By-Products, in Nanoscience Advances in CBRN Agents Detection, Information and Energy Security, P. Petkov, D. Tsiulyanu, W. Kulisch, C. Popov, Eds., Springer, Berlin, 2015, p. 199
27. D. Zgureva, S. Boycheva, *Ecolog. Eng. Environ. Protect.* **2** (2015) 12
28. R. Terzano, C. D'Alessandro, M. Spagnuolo, M. Romagnoli, L. Medici, *Clean – Soil, Air, Water* **42** (2014) 1
29. M. M. J. Treacy, J. B. Higgins, *Collection of simulated XRD powder patterns for zeolites*, Str. Comm. IZA. 5th rev. ed., Elsevier, London, 2001
30. R. Han, Y. Wang, Q. Sun, L. Wang, J. Song, X. He, C. Dou, *J. Hazard. Mater*. **175** (2010) 1056
31. Z. Ghasemi, I. Sourinejad, H. Kazemian, S. Rohani, *Rev. Aquacult.* (2016), doi: 10.1111/raq.12148
32. C. S. Cundy, P. A. Cox, *Micropor. Mesopor Mater.* **82** (2005) 1
33. P. Khemthong, S. Prayoonpokarach, J. Wittayakun, *Suranaree J. Sci. Technol.* **14** (2007) 367
34. A. Shoumkova, V. Stoyanova, *Fuel* **103** (2013) 533
35. C. W. Purnomo, C. Salim, H. Hinode, *Micropor. Mesopor. Mater.* **162** (2012) 6
36. J. Chumee, World Acad. Sci. Eng. Technol. **7** (2013) 6
37. R. Panek, M. Wdowin, W. Franus, *Springer Proc. Phys.* **154** (2014) 45
38. C. Baerlocher, R. M. Barrer, *Z. Kristallogr*. **140** (1974) 10
39. F. Miyaji, T. Murakami, Y, Suyama, *J. Ceram. Soc. Jpn*. **117** (2009) 619
40. C. Chen, T. Cheng, *Asian J. Chem.* **25** (2013) 1811
41. J. Schmelzer, J. Möller, I. Gutzow, R. Pascova, R. Müller, W. Pannhorst, *J. Non-Cryst. Solids* **183** (1995) 215
42. I. Gutzow, R. Pascova, A. Karamanov, J. Schmelzer, *J. Mater. Sci.* **33** (1998) 5265.